0013-7227/97/$03.00/0
Endocrinology

Vol. 138, No. 1
Printed in U.S.A.

Costimulation of Adenylyl Cyclase and Phospholipase C by a Mutant α_{1B}-Adrenergic Receptor Transgene Promotes Malignant Transformation of Thyroid Follicular Cells*

CATHERINE LEDENT†, JEAN-FRANÇOIS DENEF, SUSANNA COTTECCHIA‡, ROBERT LEFKOWITZ, JACQUES DUMONT, GILBERT VASSART, AND MARC PARMENTIER

IRIBHN (C.L., J.D., G.V., M.P.) and the Medical Genetics Department (G.V.), Free University of Brussels Campus Erasme; and the Histology Laboratory, University of Louvain Medical School (J.-F.D.), Brussels, Belgium; and the Departments of Medicine and Biochemistry, Howard Hughes Medical Institute, Duke University Medical Center (S.C., R.L.), Durham, North Carolina 27710

ABSTRACT

Proliferation of thyroid follicular cells is controlled by three intracellular cascades [cAMP, inositol 1,4,5-triphosphate (IP_3)/Ca^{2+}/diacylglycerol (DAG), and tyrosine kinases] that are activated by distinct extracellular signals and receptors. We had previously generated a transgenic mouse model in which the cAMP cascade was permanently stimulated in thyroid cells by an adenosine A_{2a} receptor (Tg-A_{2a}R model). In the present work, we have generated a transgenic model characterized by the chronic stimulation of both adenylyl cyclase and phospholipase C in thyroid follicular cells. The bovine thyroglobulin gene promoter was used to direct the expression of a constitutively active mutant of the α_{1B} adrenergic receptor, which is known to couple to both cascades in transfected cell lines. The expression of the transgene resulted, as expected, in the activation of phospholipase C and adenylyl cyclase, as demonstrated by the direct measurement of IP_3 and cAMP in thyroid tissue. The phenotype resulting from this dual stimulation included growth stimulation, hyperfunction, cell degeneracy attributed to the overproduction of free radicals, and the development of malignant nodules invading the capsule, muscles, and blood vessels. Differentiated metastases were found occasionally in old animals. The development of malignant lesions was more frequent and of earlier onset than in our previous Tg-A_{2a}R model, in which only the cAMP cascade was stimulated. These observations demonstrate that the cAMP and IP_3/Ca^{2+}/DAG cascades can cooperate *in vivo* toward the development of thyroid follicular cell malignancies. (*Endocrinology* **138:** 369–378, 1997)

THYROID CELL function and proliferation are controlled by factors acting on different intracellular cascades through the interaction with their specific membrane receptors (1). The main regulator of thyroid function and growth is TSH, a heterodimeric glycoprotein synthesized by pituitary thyrotrophs, and acting on a thyroid specific G protein-coupled receptor. TSH receptor activation leads to the stimulation of the cAMP cascade in all investigated mammalian species. It is well established that activation of the cAMP cascade maintains differentiation of thyrocytes and leads to the activation of both their function and proliferation (2–4). A second cascade that has been shown to promote proliferation while inducing dedifferentiation in thyroid cells in culture is the diacylglycerol (DAG)/protein kinase C branch of the phospholipase C pathway (5, 6). Phospholipase C can be stimulated in dog thyroid cells by acetylcholine (7); in human thyroid cells by ATP, bradykinin, and TRH (8, 9); and in rodent cells by α_1-adrenergic agonists (10–12). Stimulation of this cascade by the TSH receptor at high TSH concentrations has also been demonstrated in the human thyrocyte (13), but not in the dog thyrocyte (7). Stimulation of the inositol 1,4,5-triphosphate (IP_3)/Ca^{2+}/DAG cascade has been reported to promote H_2O_2 production (through the stimulation of the ill defined H_2O_2-generating system), iodide organification, and thyroid hormone synthesis (9, 14, 15). The third cascade stimulating proliferation is the tyrosine kinase/*ras*/mitogen-activated protein kinase pathway. Factors known to regulate this pathway in thyroid cells include insulin-like growth factor I, epidermal growth factor (EGF), and hepatocyte growth factor (3, 16, 17). Although EGF and hepatocyte growth factor promote proliferation and induce dedifferentiation of the thyroid cell, insulin-like growth factor I and insulin have a permissive effect on the mitogenic actions of TSH, EGF, and phorbol esters (6).

We have previously generated transgenic mouse lines expressing the adenosine A_{2a} receptor under the control of the thyroid cell-specific thyroglobulin promoter (18). Presumably through the continuous release of adenosine by thyroid tissue, the adenosine receptor expressed in thyroid cells acts

Received May 29, 1996.
Address all correspondence and requests for reprints to: Dr. Catherine Ledent, IRIBHN, Free University of Brussels Campus Erasme, 808 route de Lennik, B-1070 Brussels, Belgium.
* This work was supported by the Belgian Program on Interuniversity Poles of Attraction initiated by the Belgian State, Prime Minister's Office, Science Policy Programming; the Association Belge contre le Cancer, Télévie; the Fonds de la Recherche Scientifique Médicale; the Banque Nationale; the EEC (Biomed and Radioprotection Programs); and the Association Recherche Biomédicale et Diagnostic. All scientific responsibility is assumed by the authors.
† Chercheur Qualifié of the Fonds National de la Recherche Scientifique of Belgium.
‡ Present address: Institut de Pharmacologie et de Toxicologie, Université de Lausanne, Bugnon 27, 1005 Lausanne, Switzerland.

as a constitutive activator of the cAMP cascade, leading to the development of a toxic hyperfunctioning goiter. This transgenic model reproduces the pathogenesis and phenotype of autonomous hyperfunctional adenomas and nonautoimmune familial hyperthyroidism secondary to the permanent activation of adenylyl cyclase by constitutively active TSH receptor mutants (19, 20). A similar, although milder, phenotype was obtained in mice expressing in their thyroid a constitutively activated $G\alpha_s$, the G protein that activates adenylyl cyclase (21).

With the aim of investigating the effect of the concomitant stimulation of both the cAMP and IP_3/Ca^{2+}/DAG pathways on thyroid function and proliferation *in vivo*, we generated transgenic mouse lines expressing a mutant of the α_{1B}-adrenergic receptor that activates both cascades (22). This mutant was previously reported to be constitutively active in transfected cell lines (23) and in heart muscle cells of transgenic mice (24). As expected from the stimulation of the cAMP pathway, transgenics expressing the mutant α_{1B}-receptor partially reproduced the phenotype of the mice expressing the A_{2a}-adenosine receptor. Nevertheless, marked differences were found in the function of the gland, the evolution of the phenotype, and the frequency and timing of malignant tumor development, all changes attributed to the stimulation of phospholipase C.

Materials and Methods

Generation of transgenic mice for the bovine thyroglobulin-α_{1B}-adrenergic mutant receptor hybrid gene (Tg-α_{1B}AR)

The coding region of the mutant ($Arg^{288}Lys$, $Lys^{290}His$, $Ala^{293}Leu$) (23) hamster α_{1B}-adrenergic receptor complementary DNA (cDNA; −14 to +1745 relative to the start codon) was cloned into the polylinker of pSG5 (Stratagene, La Jolla, CA). A *Stu*I-*Sal*I restriction fragment of pSG5-α_{1B} comprising the second intron of the rabbit β-globin gene, the α_{1B} cDNA, and the polyadenylation signal was further cloned in pBluescript SK^+, downstream of a bovine thyroglobulin gene promoter fragment (−2036 to +9 bp relative to the CAP site).

Transgenic mice were generated as previously described (25). All animals were anesthetized with either avertin or ether before surgical procedures. Animals were kept at the central housing facility of the Free University of Brussels Medical School, and all procedures involving them were made in accordance with the regulations and guidelines of the Belgian State and European Union after approval by the local ethical committee. The linearized construct (1–2 pl of a 2.5 μg/ml solution) was microinjected into the pronuclei of fertilized eggs from a C57BL/6J × DBA/2J F2 cross. Screening of transgenic animals was performed by Southern blotting of DNA extracted from tail biopsies and hybridization with a bovine thyroglobulin gene promoter probe.

Hormonal, functional, and second messenger assays

Blood samples were obtained by cardiac or orbital puncture under anesthesia. Total T_4 levels were assayed on sera by standard RIA (T_4 Coat-a-Count, Clinical Assays, Cambridge, MA).

Iodide uptake was measured by counting whole thyroid glands 4 h after an ip injection of [^{125}I]NaI (15 μCi). Organification was assayed by trichloroacetic acid (5%, wt/vol) precipitation of thyroid homogenates as previously described (26). Protein-bound radioiodine was expressed as a percentage of the total iodide uptake.

For cAMP measurements, thyroid glands were collected under anesthesia and immediately immersed in boiling water. After 5 min, tissues were homogenized in a glass homogenizer, and insoluble material was removed by centrifugation. The soluble fraction was lyophilized and redissolved in water. cAMP was assayed by RIA following the kit manufacturer's instructions (cAMP125 assay system, RPA 509, Amersham, Aylesbury, UK).

For inositol phosphate determinations, thyroid glands were collected under anesthesia and flash-frozen in liquid nitrogen. They were thawed in 1 ml ice-cold 5% perchloric acid and homogenized. After centrifugation, supernatants were titrated to pH 7.5 with a solution containing 60 mM HEPES, 1.5 M KOH, and Universal Indicator. Precipitated $KClO_4$ was removed by centrifugation. Samples were purified using Amprep SAX minicolumns (RPN 1908, Amersham), and IP_3 was measured following the kit manufacturer's instructions (D-myo-inositol 1,4,5-triphosphate ^{3}H assay system, TRK 1000, Amersham).

Binding assays

Crude 40,000 × *g* membrane fractions were prepared from thyroid glands as previously described (27) and resuspended in binding buffer [50 mM Tris-HCl (pH 7.4), 5 mM EDTA, and 150 mM NaCl]. Protein content estimation was carried out using the Lowry assay, as modified by Peterson (28). Binding assays were performed on 10–100 μg membrane proteins, using the α_1-specific antagonist 2-{β-(hydroxy-3-[^{125}I]iodophenyl)ethylaminomethyl}-tetralone (2200 Ci/mmol; New England Nuclear, Hertfordshire, UK) as tracer at a saturating concentration (250 pM; reported K_d, 30–50 pM) (29). Nonspecific binding was determined in the presence of a large excess (50 μM) of prazosin (Sigma Chemical Co., St. Louis, MO). Incubations were performed for 1 h at 25 C in 250 μl binding buffer. Bound ligand was separated by filtration on GF-C membranes (Whatman, Maidstone, UK) and counted.

Northern blotting procedure

Polyadenylated RNA was isolated using the FastTrack kit (Invitrogen, San Diego, CA). After glyoxal denaturation, RNA samples (15 μg/lane) were fractionated on a 1% agarose gel in 10 mM phosphate buffer (pH 7.0) and transferred to nylon membranes (Pall Biodyne A, Glen Cove, NY) as previously described (30). DNA probes were α-^{32}P labeled by random priming (31). After hybridization and washing, the filters were autoradiographed using Amersham β-max films.

Histological and immunohistological procedures

For light microscopy, tissues were fixed by immersion for 24 h in Bouin's solution and embedded in paraffin by standard procedures. Six-micron sections were stained with hematoxylin and eosin.

For determination of the proliferation index, bromodeoxyuridine (BrdU) was injected ip (0.05 mg/g BW) 1 h before death. Thyroids were fixed in 70% ethanol-30% acetic acid, embedded in paraffin, and cut at 6-μm intervals. BrdU was detected by immunochemistry (32), using a mouse monoclonal anti-BrdU antibody (Becton Dickinson, Rutherford, NJ), a sheep biotinylated antimouse Ig serum (Amersham), and a streptavidin-biotinylated horseradish peroxidase complex (Amersham).

For semithin sections and electron microscopy, thyroids were fixed by immersion for 2 h in 2.5% glutaraldehyde (Taab, Reading, UK) in 0.1 M cacodylate buffer, dehydrated in an ethanol series of increasing strength, and embedded in LX112 (Ladd Research Industries, Burlington, VT). Sections (0.5 μm thick) were cut and stained with 1% toluidine blue for light microscopy. Ultrathin sections (30–40 nm) were cut and mounted on copper grids, stained with uranyl acetate and lead citrate, and examined on a Philips EM 301 electron microscope.

Statistical analysis

All presented data represent the mean and SD. Statistical analysis was performed by using the Graphpad Instat software. Student's *t* test was used to determine the statistical significance of the differences observed among groups for the various parameters. When SDs were significantly different between groups (as determined by the F test), therefore preventing the use of Student's *t* test, logarithmic transformation of the data was made before statistical analysis, or Welch's alternate *t* test (33) was applied instead.

Results

Generation of the mouse transgenic lines expressing the mutant α_{1B}-receptor

Six founder transgenic animals were generated, using a hybrid gene that placed the constitutively active α_{1B}-adren-

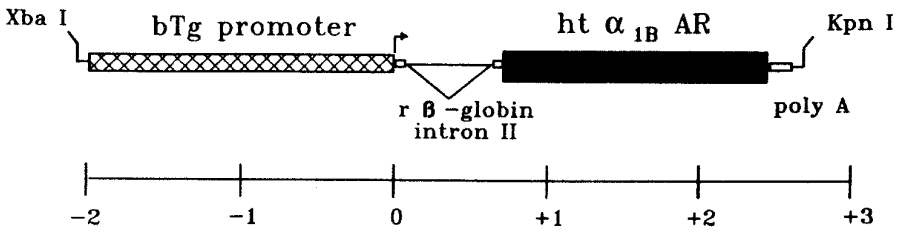

FIG. 1. Structure of the thyroglobulin-α_{1B}-adrenergic receptor transgene (Tg-α_{1B}AR) comprising the bovine thyroglobulin (bTg) promoter, the rabbit β-globin (rβ-globin) second intron, and the cDNA sequence encoding a constitutively active mutant form of the hamster α_{1B}-adrenergic receptor (ht α_{1B}AR). The scale is expressed as kilobases.

ergic receptor cDNA under control of the bovine thyroglobulin gene promoter (Fig. 1). Stable transgenic lines were established by backcrossing the founder animals (DBA/2J × C57BL/6J F2 cross) with the C57BL/6J parental line. The bovine thyroglobulin gene promoter was shown previously in a number of transgenic models to be strictly specific for the thyroid follicular cell (18, 26, 34–36). Expression of the transgene was verified by Northern blotting, using an α_{1B}-adrenergic receptor probe. α_{1B} transcripts could not be detected in the thyroid of control animals (not shown) or in that of other transgenic lines displaying undifferentiated (Tg-AgT) (26) or highly differentiated hyperfunctioning goiters (Tg-A_{2a}R; Fig. 2 (18). Abundant transcripts were found in the thyroid of transgenic animals (Fig. 2). Binding assays were also performed to detect the presence of α_{1B}-binding sites in thyroid membranes of the transgenic mice. Using the specific α_1-adrenergic receptor antagonist 2-{β-(hydroxy-3-[^{125}I]iodophenyl)ethylaminomethyl}-tetralone as ligand, a small number of binding sites was found on wild-type mouse thyroid membranes (mean ± SD, 9 ± 2 fmol/mg membrane proteins). On membranes prepared from the thyroid of transgenic animals (5 months old, line 51), α_1-binding sites were increased about 10-fold (mean ± SD, 115 ± 9 fmol/mg membrane proteins), demonstrating the functional expression of the transgene (not shown). In these conditions, the nonspecific binding was 8 ± 1 (mean ± SD) fmol/mg membrane proteins. The direct measurement of IP_3 and cAMP in thyroid tissue obtained from mice belonging to line 51 confirmed the expected dual stimulation of the IP_3/Ca^{2+}/DAG and cAMP cascades (Fig. 3).

Phenotype of transgenic mice

In all six transgenic lines, animals appeared normal up to the age of 6 months in terms of behavior and external appearance. In three lines (no. 51, 57, and 66), some of the mice developed a goiter clearly visible from external inspection at ages ranging from 6–24 months. A number of transgenics aged 1 yr or more also died prematurely. Measurements of circulating thyroid hormones demonstrated moderate to severe hyperthyroidism in most animals of lines 51 and 57 and in old animals of line 66 (see below). In the three other lines, T_4 levels were in the normal range.

Morphological analysis of the transgenic model

Animals of the six transgenic lines were killed at ages ranging from birth to 24 months, and macroscopic or microscopic abnormalities were searched for in the thyroid and other organs. Primary lesions were restricted to the thyroid, as expected from the properties of the thyroglobulin gene promoter directing the expression of the transgene. The morphological changes, when present, were grossly similar in all transgenic lines, but the timing of their appearance, and the extent and frequency of alterations were variable from one line to another. Structural abnormalities occurred earliest in line 51; the evolution was somewhat slower in line 57 and

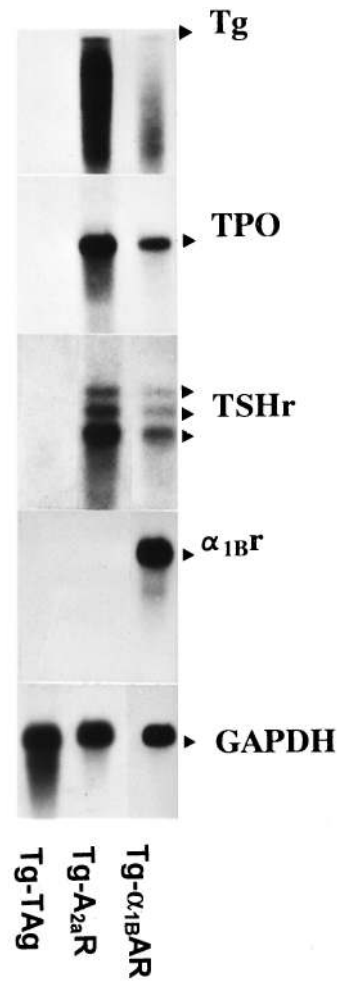

FIG. 2. Expression of the α_{1B}-adrenergic receptor and differentiation markers in transgenic animals expressing the mutant α_{1B}-adrenergic receptor (Tg-α_{1B}AR). Transcripts derived from the α_{1B} transgene and from the thyroid-specific genes thyroglobulin (Tg), thyroperoxidase (TPO), and TSH receptor (TSHr) were detected by Northern blotting. The glyceraldehyde-3-phosphate dehydrogenase (GAPDH) messenger was detected as a control. Transgenic animals expressing the large T viral oncogene (Tg-TAg) (25) and the A_{2a}-adenosine receptor (Tg-A_{2a}R) (18) were assayed simultaneously as controls for undifferentiated and hyperfunctional thyroid tissues, respectively. Each lane contains 15 μg polyadenylated RNA prepared from 4-month-old animals (line 51 for Tg-α_{1B}AR mice). Note the lack of detectable α_{1B} transcripts in Tg-TAg and Tg-A_{2a}R transgenic mice.

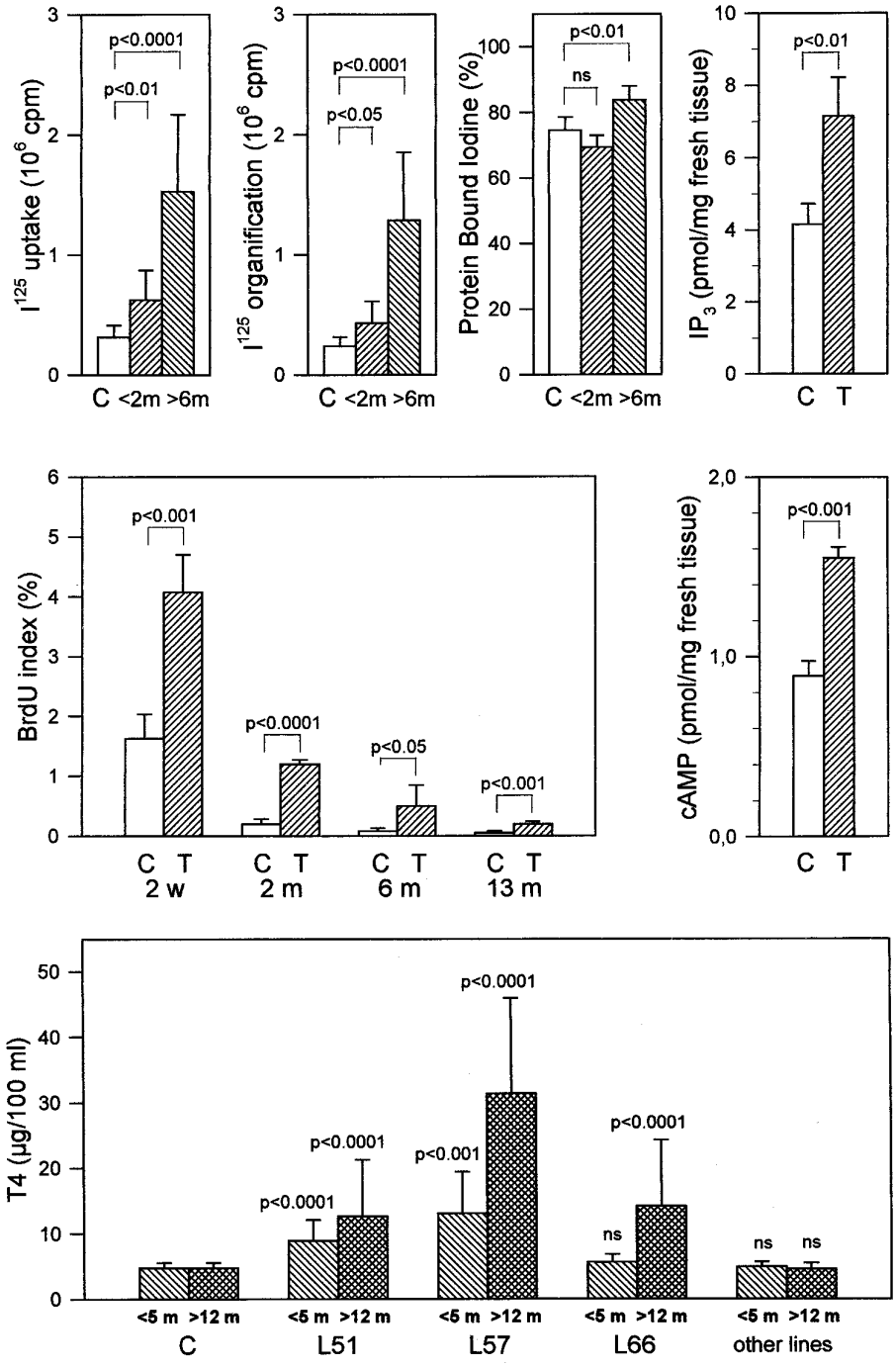

FIG. 3. Characterization of the functional and proliferative status of the thyroid gland in Tg-α_{1B}AR transgenic mice. ^{125}I uptake, ^{125}I organification, and protein-bound iodine were measured, as described in *Materials and Methods*, in 1-, 2-, 6-, and 13-month-old animals of line 51 and 1-, 3-, and 13-month-old controls. At least three animals per group were tested. The values were not significantly different between the control age groups, and the values were pooled (C; n = 9). For transgenics, the values were pooled for 1- and 2-month-old animals (<2 m; n = 6) and for 6- and 13-month-old animals (>6 m; n = 9). IP_3 levels were measured in thyroid tissue from 3.5-month-old control (C) and transgenic (T) mice from line 51 and expressed as picomoles per mg wet weight (n = 4). cAMP levels were measured by RIA on thyroids from 2.5-month-old control (C) and transgenic (T) mice from line 51 and expressed as picomoles per mg wet weight (n = 3). The BrdU index was estimated by counting the percentage of labeled nuclei in 2-week-old (2w), 2-month-old (2 m), 6-month-old (6 m), and 13-month-old (13 m) control (C) and transgenic (T) mice from line 51 (n = 4 for controls; n = 5 for transgenics). T_4 was measured in control mice (C) and transgenics (T) from the various lines (lines 51, 57, and 66 and the three other lines). Pooled values for animals less than 5 months (<5 m) and more than 12 months (>12 m) of age are given. *P* values are given for transgenic groups compared to controls (n = 6 for control groups, n = 32 and 35 for line 51, n = 13 and 13 for line 57, n = 4 and 25 for line 66, n = 12 and 15 for other lines). In all cases, the *error bar* represents the SE. Statistical analysis was made using Student's *t* test whenever SDs were not significantly different between groups. Logarithmic transformation of the data was made before statistical analysis for iodine uptake and organification. Welch's alternate *t* test (33) was used for T_4 data for lines 51, 57, and 66 and for BrdU data for 6-month-old animals.

was much delayed in line 66. In the other three lines (no. 23, 36, and 40), the morphological alterations were moderate and of late appearance. This evolution was correlated with the serum thyroid hormone levels; lines 51 and 57 were the two lines that exhibited severe hyperthyroidism from birth, whereas animals from line 66 became hyperthyroid at later stages (Fig. 3). The evolution was also correlated with the abundance of transgene-derived transcripts in the thyroid as determined by Northern blotting; transcripts were more abundant in line 51 than in line 57 or 66 (data not shown). We focused most of the analysis on the transgenic lines displaying the strongest phenotype. Functional assays were performed essentially on animals from line 51, histological data were collected mostly from animals from lines 51, 57, and 66. We will first describe the morphological changes observed in line 51. The variation in phenotypic development in the other lines will be described later.

The thyroids from mice of line 51 were increased in size from the first weeks of life, and some reached a weight of 130 mg by 12 months (control, 2 mg). The enlargement was regular and symmetrical (Fig. 4, A and B), and the general organization into follicles was preserved. The structure of the gland and the cell morphology were, nevertheless, altered. Normal thyroid tissue consists of round or ovoid follicles of

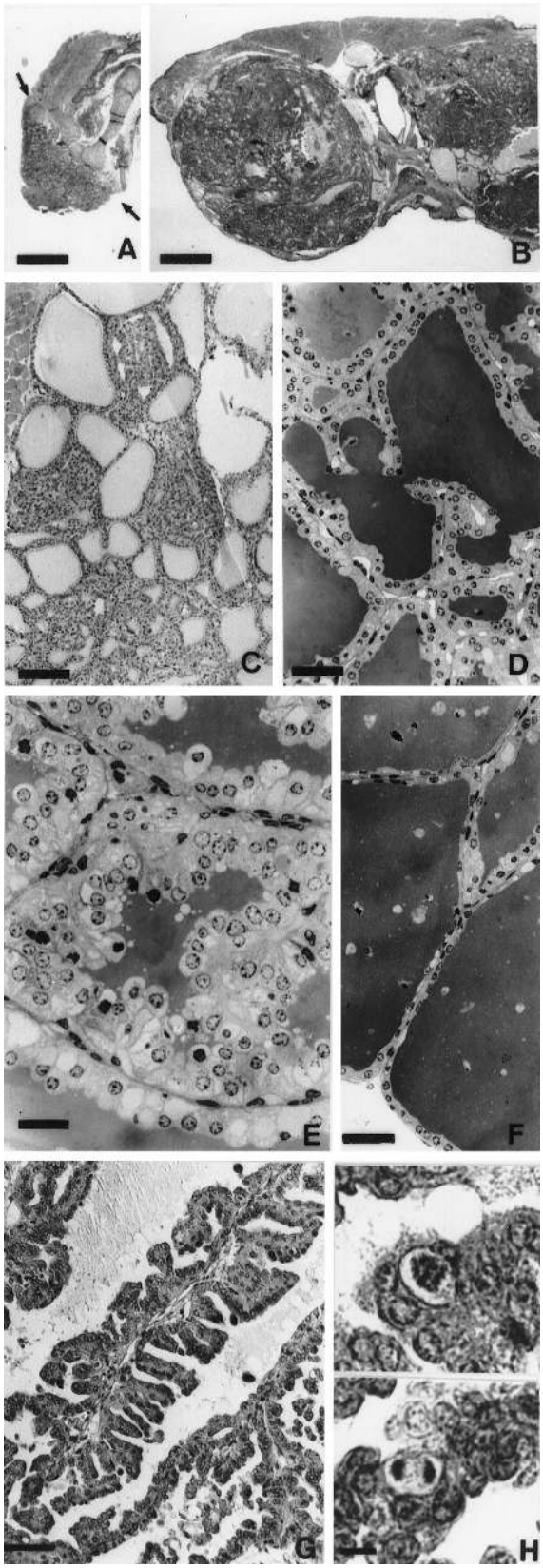

FIG. 4. Morphological pattern of the thyroid from transgenic mice expressing the mutant α_{1B}-adrenergic receptor. A and B, Gross appearance of the thyroid from a 4-month-old transgenic animal from line 51 (B) and a nontransgenic littermate (A). The *arrows* in A indicate the limits of the thyroid lobes. The nodular structure of the transgenic mouse thyroid is obvious, with the presence of areas of dense tissue and others where the follicular lumina are clearly visible. *Scale bars* = 750 μm. C, Low magnification view of the thyroid from a 1.5-month-old transgenic mouse from line 51 (fixed in Bouin's fluid and embedded in paraffin). The gland consists of follicles as well as clusters of densely packed cells forming narrow strands of branched follicular-like structures. *Scale bar* = 125 μm. D–F, Low magnification view of the thyroid from a 2.5-month-old transgenic mouse (glutaraldehyde-osmium fixed and embedded in plastic). D, The follicular lumina are unevenly divided by papillae containing a conjonctivo-vascular septum. Note the presence of pyknotic nuclei in the lumen. *Scale bar* = 50 μm. E, In some areas, the epithelium displays a pseudostratified appearance, with staggered nuclei; some of them are pyknotic, and many epithelial cells have a vacuolar appearance. *Scale bar* = 20 μm. F, At the periphery of the gland, large follicles with flattened epithelium are seen. Note the presence of cell debris inside the lumen. *Scale bar* = 40 μm. G, Partial view of a large nodule in the thyroid from a 16-month-old transgenic mouse from line 66 (fixed in Bouin's fluid and embedded in paraffin). Large follicular spaces are lined by regularly organized papillae. *Scale bar* = 50 μm. H, High magnification view of two mitoses (metaphase and anaphase) in the thyroid of a 12-month-old transgenic mouse from line 66. *Scale bar* = 10 μm.

relatively regular size and shape, lined with a cuboidal epithelium. In transgenic animals expressing the mutated α_{1B}-adrenergic receptor, clusters of densely packed cells forming narrow or branched follicular-like structures (Fig. 4C) and irregularly shaped follicles with numerous papillary infoldings (Fig. 4D) were frequent. Large follicles with weakly eosin- or periodic acid-Schiff-stained colloid were also found. Abundant cell debris, macrophages, monocytes, and neutrophils were present in the colloid. Follicles were lined by flattened epithelial cells (Fig. 4F) or by cylindrical or cuboidal cells (Fig. 4D). The cells sometimes displayed a pseudostratified organization, with nuclei found at all levels of the epithelium (Fig. 4E). Nuclei were round and regularly shaped, with a normal chromatin organization (Fig. 4E). Necrotic cells with condensed nuclei were frequently found in the epithelium or lumen (Fig. 4F). The apical region of the cells was often protruding into the lumen and was vacuolar, presenting an "empty" aspect (Fig. 4E). Ultrastructural analysis attributed this clear aspect to the presence of large cytoplasmic vesicles containing electron-lucent material (Fig. 5A) or markedly dilated cisternae of the rough endoplasmic reticulum (Fig. 5B) that sometimes occupied most of the cell volume. Electron-dense inclusions with homogeneous or heterogeneous contents were frequent (Fig. 5, A and B). Mitoses (Fig. 5H) were found with a relatively high frequency (they are extremely rare in the thyroid of adult controls). Bromodeoxyuridine incorporation confirmed the higher proliferation rate of thyroid cells in transgenic animals compared to controls (Fig. 3). Vascularization of the thyroid was normal or moderately increased compared to that in control animals.

The organization of the gland became increasingly heterogeneous with age, with the appearance and growth of actively proliferating nodules (Figs. 4, C and B, and 6A). The mean size and number of the nodules increased with the age of the animals, and their higher proliferation rate was confirmed by BrdU incorporation (not shown). The nodules were usually homogeneous and displayed various architectural and differentiation patterns. They were generally more

dense than the surrounding tissue, and the structural organization included follicular, microfollicular, papillary, trabecular, and solid masses, with a higher frequency of papillary structures. The cell morphology was sometimes similar to that of the surrounding thyroid gland, but most of the nodules completely lost their clear cell aspect. In large nodules, foci of cells were found, with large nuclei adopting morphological criteria that characterize human papillary carcinomas (ground glass aspect, pseudoinclusions; Fig. 6B). In a few cases, all morphological criteria of thyroid follicular cell differentiation were lost; spindle cell foci were found, without formation of identifiable follicles (Fig. 6C). The nodules were never encapsulated. They frequently acquired structural characteristics that are considered malignant criteria for human thyroid tumors. In these cases, the capsule surrounding the gland became markedly thickened, irregular, and frequently invaded by the growing nodule (Fig. 6A); local invasion also involved muscular tissue. Some of the nodules appeared highly vascularized, to the point that areas of the gland were transformed into vascular lakes filled with digitations of thyroid tissue (Fig. 6D). When this feature was encountered, invasion of blood vessels, vascular emboli in large capsular or pericapsular veins (Fig. 6E), as well as differentiated lung metastases (Fig. 6F) were frequently observed. The overall frequency of lung metastases was estimated to be 20% in animals over 12 months of age.

As stated above, the morphological phenotype of the animals in line 57 was grossly similar to that in line 51, but delayed. The clear cell aspect was present from the first weeks of life, but was less obvious. Papillary proliferation was found in early stages, and nodules with various architectures appeared with a high frequency in older animals. In line 66, the morphology of the thyroid was normal during the first months, but nodules (often solitary) appeared in almost all animals and became typically much larger than those in lines 51 and 57 (the morphology of one of these nodules is shown in Fig. 4G). In animals more than 15 months of age, the largest goiters were found in mice derived from line 66, and these goiters resulted generally from a single large nodule per lobe. Some of the most malignant phenotypes were also found in these mice (Fig. 6, C, D, and E), and the circulating T_4 levels generally correlated with the size of the goiter. For the three other transgenic lines, mild alterations were found in old animals, including a slight increase in thyroid size and heterogeneity in follicle size and shape (not shown). Small papillary nodules were occasionally found. None of these animals was hyperthyroid.

Functional and proliferative status of the thyroid gland

Thyroid hormone levels reflected the functional activity of the gland; they were elevated in most animals from lines 51 and 57 (Fig. 3). In line 51, young mice were hyperthyroid, but older mice with large nodules were characterized by a wider range of T_4 measurements, presumably resulting from the functional properties of the individual nodules. As a result, the mean T_4 level in line 51 exhibited only a mild increase with age (Fig. 3). In line 57, young animals were hyperthyroid as well, and mean T_4 levels increased strongly with age and the development of secondary nodules (Fig. 3). In line 66, T_4 levels were normal during the first months of age and increased significantly in older animals bearing large nodules (Fig. 3), suggesting that in this line, most nodules were indeed functional.

Iodide uptake and organification were estimated after ip injection of [^{125}I]NaI in animals (1, 2, 6, and 13 months) belonging to line 51. Uptake and organification were increased compared to those in controls, in proportion to the weight of the gland (Fig. 3). The efficiency of iodine incorporation into iodoproteins (protein-bound radioiodine) was similar in transgenic and control animals at all ages (Fig. 3).

The proliferation rate was assayed by measuring the percentage of cells labeled after a single ip injection of BrdU. This measurement was made on animals from line 51 at different ages (Fig. 3). Compared with control animals, which show very little thyroid cell turnover after the first few weeks of life, the labeling index of transgenic thyroids was maintained at a higher level throughout life, although it decreased progressively.

The expression level of thyroid-specific genes was investigated by Northern blotting in the thyroids of mice transgenic for the mutant α_{1B}-adrenergic receptor and was compared to that in other transgenic lines characterized by dedifferentiation (simian virus 40 large T antigen expression, Tg-TAg) or hyperfunctioning (A_{2a}-adenosine receptor expression, Tg-A_{2a}R) of the thyroid cell (Fig. 2). Controls were tested in parallel, but the amount of messenger RNA obtained was much lower than that in the transgenic lines, and the results are not shown in the figure. Thyroglobulin, thyroperoxidase, and TSH receptor transcripts were all present in the thyroid of Tg-α_{1B}AR mice, although they were less abundant than in Tg-A_{2a}R mice. Compared to controls, there was an increase in thyroperoxidase and TSH receptor transcripts and a decrease in thyroglobulin transcripts (not shown). The three differentiation markers were undetectable in Tg-TAg mice, as previously described (26).

Discussion

In our previous Tg-A_{2a}R transgenic mouse model, the expression of the wild-type A_{2a}-adenosine receptor under control of the bovine thyroglobulin gene promoter resulted in a permanent activation of the cAMP cascade. This led to a strong stimulation of thyroid cell function and the development of a large goiter, confirming the main role of this cascade in the *in vivo* control of thyroid cell function and proliferation (18). In the long run, focal malignant lesions were found, demonstrating that wild type G_s-coupled receptors can act as oncogenic proteins, when ectopically and/or overexpressed (Ledent, C., unpublished observations). The A_{2a}-adenosine receptor has not been reported to be coupled to signaling pathways other than adenylyl cyclase, and we verified experimentally that this receptor did not activate phospholipase C (Ledent, C., unpublished observations). In humans and rodents, some of the thyroid cell functions (H_2O_2 generation and incorporation of iodine into iodoproteins) are under the control of the IP_3/Ca^{2+}/DAG cascade. The DAG/protein kinase C arm of this cascade also promotes proliferation and dedifferentiation of the thyroid cell *in vitro* (6), and the TSH receptor stimulates both adenylyl

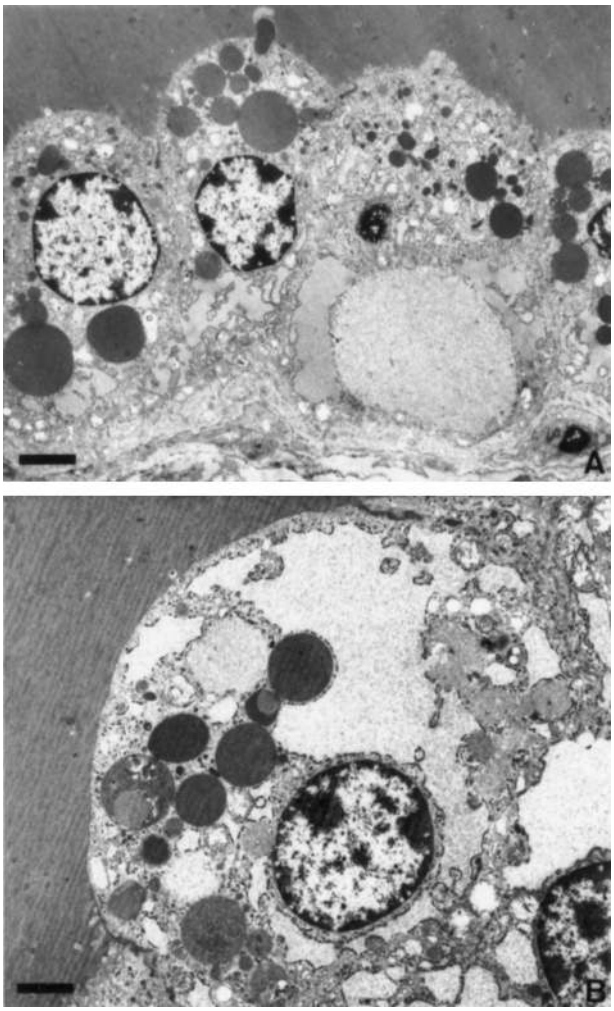

FIG. 5. Ultrastructure of the thyroid cells in a 5.5-month-old transgenic mouse from line 51 (glutaraldehyde-osmium fixed and embedded in plastic). A, Large electron-lucent vesicles are found in the cytoplasm in association with numerous dense bodies. *Scale bar* = 2 μm. B, In cells budding into the lumen, cisternae of rough endoplasmic reticulum are highly dilated. Note the presence of heterogeneous dense bodies. *Scale bar* = 1.2 μm.

cyclase and phospholipase C in human thyrocytes. To verify *in vivo* the roles attributed to phospholipase C activation in thyroid follicular cells, we decided to generate a transgenic model in which both the cAMP and IP_3/Ca^{2+}/DAG cascades would be stimulated permanently.

Constitutive activity of G protein-coupled receptors was first described (23) for an α_{1B}-adrenergic receptor mutated in the third cytoplasmic loop ($Arg^{288}Lys$, $Lys^{290}His$, and $Ala^{293}Leu$). This mutant receptor was characterized by a marked increase in affinity for agonists (but not antagonists) and by a basal coupling to G_q in the absence of agonists (23). Expression in NIH-3T3 cells demonstrated the transforming potential of the mutant (29). This mutant was recently used to generate transgenic mice under the control of the α-myosin heavy chain, leading to heart muscle-specific expression and cardiac hypertrophy (24). The Ala^{293}>Leu mutation has been shown to contribute to the constitutive properties of this mutant receptor, as any amino acid substitution at position 293 led to increased basal activity (37). Although their main signaling pathway is through phospholipase C, the α_{1B} receptor, its mutants, as well as other α_1 receptor subtypes were shown to also activate the cAMP pathway in tissues or transfected cell lines (22, 38–40) (Cotecchia, S., unpublished observations) by direct (G_s activation) and indirect mechanisms.

α_{1B} mutant receptors, therefore, appeared as an ideal means of constitutively activating phospholipase C and adenylyl cyclase in transgenic mice. A hybrid gene was engineered by placing the mutant receptor (23, 41) under the control of the bovine thyroglobulin gene promoter. This Tg-α_{1B}AR construct was used to generate six transgenic lines. The expression of the transgene was confirmed by Northern blotting, and the presence of functional α_1-adrenergic receptors in thyroid tissue was determined by ligand binding assays. Direct measurements of cAMP and IP_3 levels in the thyroids of transgenic animals confirmed the dual stimulation of adenylyl cyclase and phospholipase C by the mutant receptor. The stimulation of the cAMP pathway, however, was weaker than that in our previous Tg-A_{2a}R model (18). This was not unexpected from a mutant receptor whose main coupling is through the phospholipase C pathway.

Mice belonging to the Tg-α_{1B}AR lines developed a phenotype including hyperthyroidism and the development of thyroid nodules, ultimately leading to malignant tumors. This phenotype, however, was quite variable in its intensity and in the timing of its appearance from one line to another. This variability was correlated to the level of expression of the transgene. We reported previously, using the bacterial chloramphenicol acetyltransferase gene as reporter gene, that the expression from the thyroglobulin gene promoter in transgenic mice is highly variable from line to line (34). Variability in the expression level and in the severity of the phenotype was observed for other transgenes expressed under the dependence of the same promoter (18, 26, 36). Such variability is believed to be dependent on the site of integration of the transgene in the mouse genome.

Animals from lines 51 and 57 were markedly hyperthyroid from birth, whereas mice from line 66 developed hyperthyroidism only in association with the growth of large nodules in their thyroid. The serum T_4 values of young animals (<5 months old) did not reach the high levels that characterized Tg-A_{2a}R mice (18), in accordance with the lower stimulation of the cAMP cascade in the Tg-α_{1B}AR model. Nevertheless, with the development of nodules in older animals (>5 months old) from lines 57 and 66, T_4 values reached levels similar to those in the Tg-A_{2a}R model. The Tg-α_{1B}AR mice also exhibited a high capacity for taking up iodine and incorporating it into iodoproteins. As expected and similar to the situation in our previous Tg-A_{2a}R model, activation of the cAMP cascade by the mutant α_{1B}-adrenergic receptor resulted in stimulation of thyroid function.

There were, however, marked differences between the present Tg-α_{1B}AR mice and our previous Tg-A_{2a}R model. The thyroids from lines 51 and 57 were characterized by clear follicular cells filled with large vacuoles resulting from organellar degeneration and by a high frequency of cell necrosis. This was never encountered in the Tg-A_{2a}R model, in which the epithelium lining the follicles was normal, and

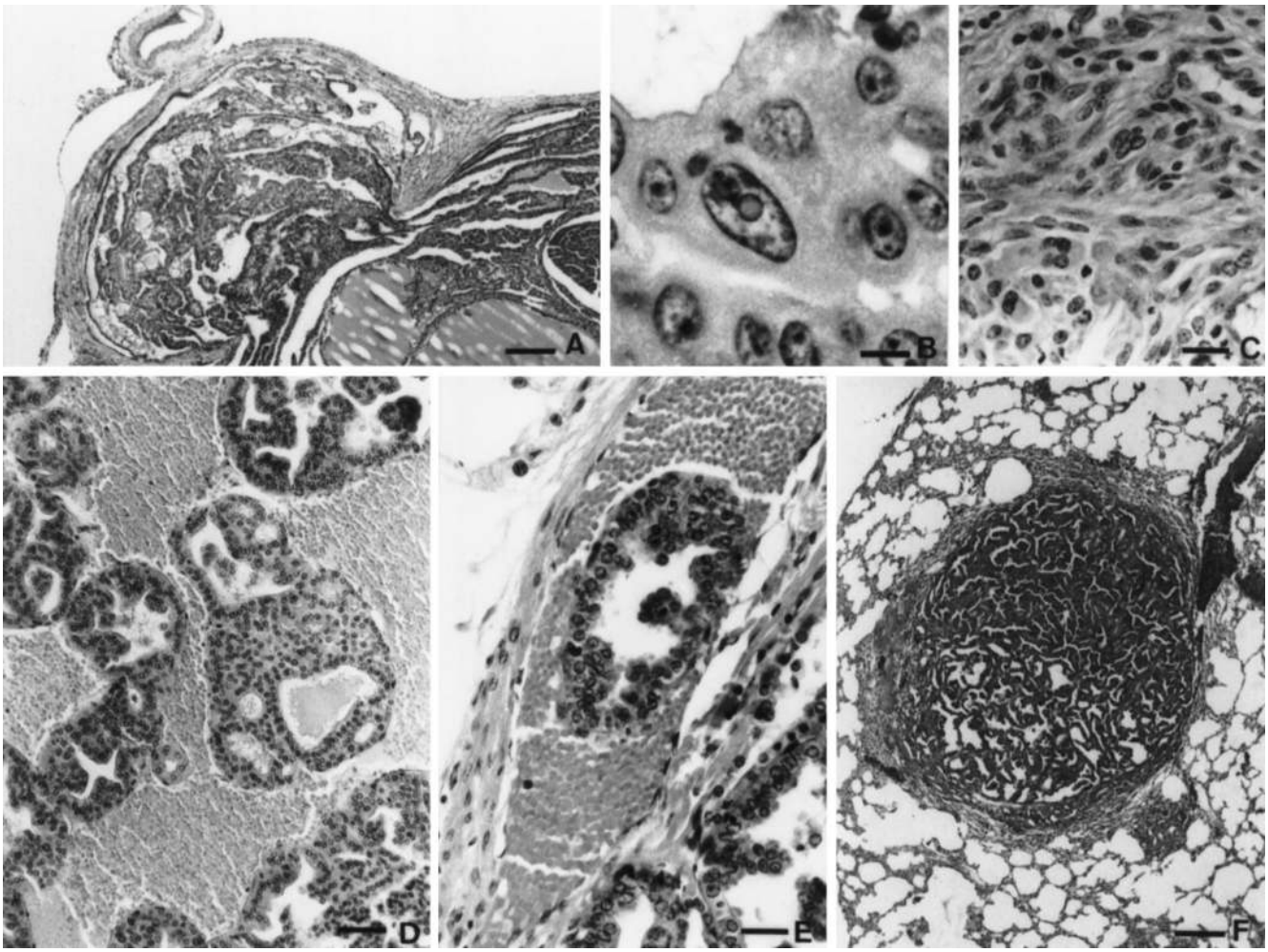

FIG. 6. Views of the thyroid from transgenic mice expressing the mutant α_{1B}-adrenergic receptor (fixed in Bouin's fluid and embedded in paraffin). A, A nodule has penetrated the capsule in the gland of a 12-month-old animal from line 51. Note the thickening of the interrupted original capsule and the formation of a new capsule around the invading tissue. *Scale bar* = 150 μm. B, Foci of cells with large irregular nuclei with pseudoinclusions and prominent nucleoli observed in a 3-month-old mouse from line 57. *Scale bar* = 10 μm. C, In some areas, cells have a spindle-like shape and do not form follicles (within a large nodule of a 17-month-old mouse from line 66). *Scale bar* = 25 μm. D, In highly vascularized nodules, blood vessels form vascular lakes containing digitations of thyroid tissue (17-month-old mouse from line 66). *Scale bar* = 65 μm. E, In the capsule, vascular permeation of glandular tissue is observed (16-month-old mouse from line 66). *Scale bar* = 30 μm. F, Partial view of the lung of a 19-month-old mouse from line 66, showing one of the multiple differentiated metastases deriving from the thyroid tumor that were found in this animal. *Scale bar* = 200 μm.

necrosis was exceptional. Such degeneration of follicular cells has been shown to occur in situations characterized by an excessive production of free radicals (42). This aspect of the phenotype can be attributed to the stimulation of the IP_3/Ca^{2+}/DAG cascade, in agreement with the *in vitro* demonstration that phospholipase C stimulates the H_2O_2 generation system and iodine organification in thyroid cells (9, 43). Cell degeneracy was prominent in line 51, where cell necrosis appeared to balance proliferation; despite a high index of bromodeoxyuridine incorporation, the goiters did not grow as large as in other lines (no. 57 and 66). In line 51, many nodules that ultimately grew to a large size had often lost their clear cell morphology, probably as a consequence of a selection process. In support of this view, the T_4 level in animals from line 51 did not correlate with the size of the gland, suggesting that most of the large nodules were poorly active. In animals from line 57, cell degeneracy was less pronounced, and the selection against functional activity was reduced, as T_4 levels increased readily with the development of nodules. Clear cells were not observed in young animals from the other lines in agreement with their overall milder phenotype.

Another marked difference with the Tg-A_{2a}R model was the rapid development of nodules, and their frequent evolution toward malignancy. Multiple nodules developed in lines 51 and 57, whereas animals from line 66 developed late, but very aggressive, functional nodules. Vascular invasion and lung metastases were relatively frequent in old animals. The higher malignancy of this model compared to that of the Tg-A_{2a}R mice is presumably due to concomitant stimulation of phospholipase C and adenylyl cyclase. It has been shown *in vitro* that the DAG/protein kinase C arm of the cascade, if stimulated long enough, can promote the growth and

dedifferentiation of thyroid cells (6). We demonstrate here *in vivo* that chronic phospholipase C stimulation can cooperate with the cAMP pathway toward proliferation and transformation, without affecting the differentiation of thyroid cells.

In conclusion, this work demonstrates that the permanent activation of both phospholipase C and adenylyl cyclase in the thyroid follicular cell of transgenic mice promotes as phenotypic characteristics stimulation of function, induction of cell degeneration attributed to the overproduction of free radicals, stimulation of proliferation, and tumor growth. Signs of malignancy, including vascular invasion, appear more frequently and earlier than in previous transgenic models. The present mouse lines constitute the most aggressive transgenic model of differentiated thyroid tumors to date, as the result of the expression of a single transgene. This model also demonstrates that membrane receptors coupled to phospholipase C may cooperate with the simultaneous stimulation of the cAMP cascade and contribute to the development of thyroid follicular cell malignancies. The possible relevance of our transgenic model for human cancer will require a search for genetic events (such as mutations in receptor genes) resulting in constitutive stimulation of the phospholipase C pathway in thyroid tumors.

Acknowledgments

We thank E. Bressy, J. Conti, C. Massart, and V. Schwam for expert technical assistance, and L. F. Allen, C. Gervy, A. Radulescu, and S. Swillens for helpful discussions. We are grateful to J. Van Sande for the cAMP and IP_3 assays in COS-7 cells.

References

1. **Stringer BMJ, Wynford-Thomas D** 1989 Control of thyroid follicular cell proliferation-molecular aspects. In: Wynford-Thomas D, Williams ED (eds) Thyroid Tumours: Molecular Basis of Pathogenesis. Churchill Livingstone, London, pp 91–122
2. **Roger PP, Hotimsky A, Moreau C, Dumont JE** 1982 Stimulation by thyrotropin, cholera toxin and dibutyryl cyclic AMP of the multiplication of differentiated thyroid cells *in vitro*. Mol Cell Endocrinol 26:165–176
3. **Dumont JE, Lamy F, Roger PP, Maenhaut C** 1992 Physiological and pathological regulation of thyroid cell proliferation and differentiation by thyrotropin and other factors. Physiol Rev 72:667–697
4. **Ledent C, Parmentier M, Maenhaut C, Taton M, Pirson I, Lamy F, Roger PP, Dumont JE** 1991 The TSH cyclic AMP cascade in the control of thyroid cell proliferation: the story of a concept. Thyroidology 3:97–102
5. **Bachrach LK, Eggo MC, Mak WW, Burrow GN** 1985 Phorbol esters stimulate growth and inhibit differentiation in cultured thyroid cells. Endocrinology 116:1603–1609
6. **Roger PP, Reuse S, Servais P, Van Heuverswyn B, Dumont JE** 1986 Stimulation of cell proliferation and inhibition of differentiation expression by tumor-promoting phorbol esters in dog thyroid cells in primary culture. Cancer Res 46:898–906
7. **Graff I, Mockel J, Laurent E, Erneux C, Dumont JE** 1987 Carbachol and sodium fluoride, but not TSH, stimulate the generation of inositol phosphates in the dog thyroid. FEBS Lett 210:204–210
8. **Raspe E, Laurent E, Andry G, Dumont JE** 1991 ATP, bradykinin, TRH and TSH activate the Ca^{2+}-phosphatidylinositol cascade of human thyrocytes in primary culture. Mol Cell Endocrinol 81:175–183
9. **Corvilain B, Laurent E, Lecomte M, Van Sande J, Dumont JE** 1994 Role of the cyclic adenosine 3′,5′-monophosphate and the phosphatidylinositol-Ca^{2+} cascades in mediating the effects of thyrotropin and iodide on hormone synthesis and secretion in human thyroid slices. J Clin Endocrinol Metab 79:152–159
10. **Muraki T, Uzumaki H, Nakadate T, Kato R** 1982 Involvement of α_1-adrenergic receptors in the inhibitory effect of catecholamines on the thyrotropin-induced release of thyroxine by the mouse thyroid. Endocrinology 110:51–54
11. **Corda D, Marcocci C, Kohn LD, Axelrod J, Luini A** 1985 Association of the changes in cytosolic Ca^{2+} and iodide efflux induced by thyrotropin and by the stimulation of alpha 1-adrenergic receptors in cultured rat thyroid cells. J Biol Chem 260:9230–9236
12. **Meucci O, Scorziello A, Avallone A, Ventra C, Grimaldi M, Berlingieri MT, Fusco A, Schettini G** 1994 α_{1A}- and α_{1B}-adrenergic receptors mediate the effect of norepinephrine on cytosolic calcium levels in rat PC C13 thyroid cells: thyrotropin modulation of alpha 1B-linked response via a adenosine 3′,5′-monophosphate-protein kinase-A-dependent pathway. Endocrinology 134:424–431
13. **Laurent E, Mockel, J, Van Sande J, Graff I, Dumont JE** 1987 Dual activation by thyrotropin of the phospholipase C and cyclic AMP cascades in human thyroid. Mol Cell Endocrinol 52:273–278
14. **Bjorkman U, Erkholm R** 1984 Generation of H_2O_2 in isolated porcine thyroid follicles. Endocrinology 115:392–398
15. **Corvilain B, Van Sande J, Laurent E, Dumont JE** 1991 The H_2O_2-generating system modulates protein iodination and the activity of the pentose phosphate pathway in dog thyroid. Endocrinology 128:779–785
16. **Dumont JE, Vassart G, Refetoff S** 1989 Thyroid disorders. In: The Scriver CR, Beauded A, Sly WS, Valle D (eds) Metabolic Basis of Inherited Diseases. McGraw-Hill, New York, pp 1843–1879
17. **Dumont JE, Jauniaux JC, Roger PP** 1989 The cyclic AMP-mediated stimulation of proliferation. Trends Biochem Sci 14:67–71
18. **Ledent C, Dumont JE, Vassart G, Parmentier M** 1992 Thyroid expression of an A2 adenosine receptor transgene induces thyroid hyperplasia and hyperthyroidism. EMBO J 11:537–542
19. **Parma J, Duprez L, Van Sande J, Cochaux P, Gervy C, Mockel J, Dumont JE, Vassart G** 1993 Somatic mutations in the thyrotropin receptor gene cause hyperfunctioning thyroid adenomas. Nature 365:649–651
20. **Duprez L, Parma J, Van Sande J, Allgeier A, Leclere J, Schvartz C, Delisle MJ, Decoulx M, Orgiazzi J, Dumont JE, Vassart G** 1994 Germline mutations in the thyrotropin receptor gene cause non-autoimmune autosomal dominant hyperthyroidism. Nat Genet 7:396–401
21. **Michiels FM, Caillou B, Talbot M, Dessarps Freichey F, Maunoury MT, Schlumberger M, Mercken L, Monier R, Feunteun J** 1994 Oncogenic potential of guanine nucleotide stimulatory factor alpha subunit in thyroid glands of transgenic mice. Proc Natl Acad Sci USA 91:10488–10492
22. **Horie K, Itoh H, Tsujimoto G** 1995 Hamster alpha 1B-adrenergic receptor directly activates Gs in the transfected Chinese hamster ovary cells. Mol Pharmacol 48:392–400
23. **Cotecchia S, Exum S, Caron MG, Lefkowitz RJ** 1990 Regions of the alpha 1-adrenergic receptor involved in coupling to phosphatidylinositol hydrolysis and enhanced sensitivity of biological function. Proc Natl Acad Sci USA 87:2896–2900
24. **Milano CA, Dolber PC, Rockman HA, Bond RA, Venable ME, Allen LF, Lefkowitz RJ** 1994 Myocardial expression of a constitutively active alpha 1B-adrenergic receptor in transgenic mice induces cardiac hypertrophy. Proc Natl Acad Sci USA 91:10109–10113
25. **Hogan BLM, Costantin F, Lacy E** 1986 Manipulating the Mouse Embryo: A Laboratory Manual. Cold Spring Harbor Laboratory, Cold Spring Harbor
26. **Ledent C, Dumont J, Vassart G, Parmentier M** 1991 Thyroid adenocarcinomas secondary to tissue-specific expression of simian virus-40 large T-antigen in transgenic mice. Endocrinology 129:1391–1401
27. **Bruns RF, Lu GH, Pugsley TA** 1986 Characterization of the A2 adenosine receptor labeled by [^{3}H]NECA in rat striatal membranes. Mol Pharmacol 29:331–346
28. **Peterson GL** 1977 A simplification of protein assay method of Lowry which is generally applicable. Anal Biochem 83:346–356
29. **Allen LF, Lefkowitz RJ, Caron MG, Cotecchia S** 1991 G-Protein-coupled receptor genes as protooncogenes: constitutively activating mutation of the alpha 1B-adrenergic receptor enhances mitogenesis and tumorigenicity. Proc Natl Acad Sci USA 88:11354–11358
30. **Thomas PS** 1980 Hybridization of denaturated RNA and small DNA fragments transferred to nitrocellulose. Proc Natl Acad Sci USA 77:5201–5205
31. **Feinberg AP, Vogelstein B** 1983 A technique for radiolabelling DNA restriction endonucleases fragments to high specific activity. Anal Biochem 132:6–13
32. **Schutte B, Reynders MMJ, Bosman FT, Blijham GH** 1987 Effect of tissue fixation on anti-bromodeoxyuridine immunochemistry. J Histochem Cytochem 35:1343–1345
33. **Welch BL** 1937 The significance of the difference between two means when the population variances are unequal. Biometrika 29:350–361
34. **Ledent C, Parmentier M, Vassart G** 1990 Tissue-specific expression and methylation of a thyroglobulin-chloramphenicol acetyltransferase fusion gene in transgenic mice. Proc Natl Acad Sci USA 87:6176–6180
35. **Wallace H, Ledent C, Vassart G, Bishop JO, Al-Shawi R** 1991 Specific ablation of thyroid follicle cells in adult transgenic mice. Endocrinology 129:3217–3226
36. **Ledent C, Marcotte A, Dumont JE, Vassart G, Parmentier M** 1995 Differentiated carcinomas develop as a consequence of the thyroid specific expression of a thyroglobulin-human papillomavirus type 16 E7 transgene. Oncogene 10:1789–1797
37. **Kjelsberg MA, Cotecchia S, Ostrowski J, Caron MG, Lefkowitz RJ** 1992 Constitutive activation of the alpha 1B-adrenergic receptor by all amino acid substitutions at a single site. Evidence for a region which constrains receptor activation. J Biol Chem 267:1430–1433
38. **Perez DM, DeYoung MB, Graham RM** 1993 Coupling of expressed alpha 1B-

and alpha 1D-adrenergic receptor to multiple signaling pathways is both G protein and cell type specific. Mol Pharmacol 44:784–795

39. **Cotecchia S, Kobilka BK, Daniel KW, Nolan RD, Lapetina EY, Caron MG, Lefkowitz RJ, Regan JW** 1990 Multiple second messenger pathways of alpha-adrenergic receptor subtypes expressed in eukaryotic cells. J Biol Chem 265:63–69
40. **Nomura T, Kondo H, Hasegawa S, Watanabe T, Yokoyama R, Ukai K, Tachibana M, Sumi Ichinose C, Nomura H, Hagino Y** 1993 Alpha 1B-adrenoceptor-mediated stimulation of Ca^{2+} mobilization and cAMP accumulation in isolated rat hepatocytes. Eur J Pharmacol 246:113–120
41. **Cotecchia S, Schwinn DA, Randall RR, Lefkowitz RJ, Caron MG, Kobilka BK** 1988 Molecular cloning and expression of the cDNA for the hamster alpha 1-adrenergic receptor. Proc Natl Acad Sci USA 85:7159–7163
42. **Mahmoud I, Colin I, Many MC, Denef JF** 1986 Direct toxic effect of iodide in excess on iodine-deficient thyroid glands: epithelial necrosis and inflammation associated with lipofuscin accumulation. Exp Mol Pathol 44:259–271
43. **Dumont JE, Corvilain B, Contempre B** 1994 The biochemistry of endemic cretinism: roles of iodine and selenium deficiency and goitrogens. Mol Cell Endocrinol 100:163–166